Coherent beam transformations using multimode waveguides

X. Zhu*, A. Schülzgen, H. Li, H. Wei, J. V. Moloney, and N. Peyghambarian

College of Optical Sciences, University of Arizona, 1641 East University Boulevard, Tucson, Arizona 85721, USA
*xszhu@email.arizona.edu

Abstract: Physical insights and characteristics of beam transformations based on multimode interference (MMI) in multimode waveguides are illuminated and analyzed. Our calculations show that, utilizing a short piece of cylindrical multimode waveguide, an input Gaussian beam can be readily transformed to frequently desired beams including top-hat, donut-shaped, taper-shaped, and Bessel-like beams in the Fresnel or the Fraunhofer diffraction range, or even in both ranges. This is a consequence of diffractive propagation of the field exiting the waveguide. The performance of the beam shaper based on MMI can be controlled via tailoring the dimensions of the multimode waveguide or changing the signal wavelength. This beam shaping technique is investigated experimentally using monolithic fiber devices consisting of a short piece of multimode fiber (~ 10 mm long) and a single-mode signal delivery fiber.

OCIS codes: (350.6980) Transforms; (060.2310) Fiber optics; (130.2790) Guided waves; (260.1960) Diffraction theory; (260.3160) Interferences; (110.2945) Illumination design; (350.5500) Propagating.

References and links

1. F. Dickey, and S. Holswade, eds., *Laser Beam Shaping: Theory and Techniques* (New York: Marcel Dekker, 2000).
2. F. Dickey, D. Shealy, and S. Holswade, eds., *Laser Beam Shaping Applications* (New York: Marcel Dekker, 2005).
3. Y. Matsuura, M. Miyagi, A. German, L. Nagli, and A. Katzir, "Silver-halide fiber tip as a beam homogenizer for infrared hollow waveguides," Opt. Lett. **22**(17), 1308–1310 (1997).
4. Y. Matsuura, D. Akiyama, and M. Miyagi, "Beam homogenizer for hollow-fiber delivery system of excimer laser light," Appl. Opt. **42**(18), 3505–3508 (2003).
5. J. R. Hayes, J. C. Flanagan, T. M. Monro, D. J. Richardson, P. Grunewald, and R. Allott, "Square core jacketed air-clad fiber," Opt. Express **14**(22), 10345–10350 (2006).
6. X. Gu, W. Mohammed, L. Qian, and P. W. E. Smith, "All-fiber laser beam shaping using a long-period grating," IEEE Photon. Technol. Lett. **20**(13), 1130–1132 (2008).
7. Z. Tian, M. Nix, and S. S.-H. Yam, "Laser beam shaping using a single-mode fiber abrupt taper," Opt. Lett. **34**(3), 229–231 (2009).
8. Y. O. Yilmaz, A. Mehta, W. S. Mohammed, and E. G. Johnson, "Fiber-optic beam shaper based on multimode interference," Opt. Lett. **32**(21), 3170–3172 (2007).
9. X. Zhu, A. Schülzgen, L. Li, and N. Peyghambarian, "Generation of controllable nondiffracting beams using multimode optical fibers," Appl. Phys. Lett. **94**(20), 201102 (2009).
10. X. Zhu, A. Schülzgen, H. Li, L. Li, L. Han, J. V. Moloney, and N. Peyghambarian, "Detailed investigation of self-imaging in large-core multimode optical fibers for application in fiber lasers and amplifiers," Opt. Express **16**(21), 16632–16645 (2008).
11. W. S. Mohammed, A. Mehta, and E. G. Johnson, "Wavelength tunable fiber lens based on multimode interference," J. Lightwave Technol. **22**(2), 469–477 (2004).
12. A. Mehta, W. S. Mohammed, and E. G. Johnson, "Multimode interference-based fiber-optic displacement sensor," IEEE Photon. Technol. Lett. **15**(8), 1129–1131 (2003).
13. R. Selvas, I. Torres-Gomez, A. Martinez-Rios, J. A. Alvarez-Chavez, D. A. May-Arrioja, P. Likamwa, A. Mehta, and E. G. Johnson, "Wavelength tuning of fiber lasers using multimode interference effects," Opt. Express **13**(23), 9439–9445 (2005).
14. X. Zhu, A. Schülzgen, H. Li, L. Li, Q. Wang, S. Suzuki, V. L. Temyanko, J. V. Moloney, and N. Peyghambarian, "Single-transverse-mode output from a fiber laser based on multimode interference," Opt. Lett. **33**(9), 908–910 (2008).

#120821 - $15.00 USD Received 7 Dec 2009; revised 23 Feb 2010; accepted 28 Feb 2010; published 26 Mar 2010

15. X. Zhu, A. Schülzgen, H. Li, L. Li, V. L. Temyanko, J. V. Moloney, and N. Peyghambarian, "High power fiber lasers and amplifiers based on multimode interference," IEEE J. Sel. Top. Quantum Electron. **15**(1), 71–78 (2009).
16. X. Zhu, "Multimode interference in optical fibers and its applications in fiber lasers and amplifiers," Phd's dissertation, University of Arizona (2008).
17. E. Sziklas, and A. Siegman, "Diffraction calculations using fast Fourier transform methods," Proc. IEEE **62**(3), 410–412 (1974).
18. H. Li, M. Brio, L. Li, A. Schülzgen, N. Peyghambarian, and J. V. Moloney, "Multimode interference in circular step-index fibers studies with the mode expansion approach," J. Opt. Soc. Am. B **24**(10), 2707 (2007).

1. Introduction

Due to the increasing demand of laser beams with intensity profiles other than Gaussian or with specific multimode distributions for various practical applications, such as laser processing, lithography, fiber injection, medical applications, and laboratory research, laser beam shaping that redistributes the irradiance and phase of an incident beam to achieve a desired intensity distribution has been intensively studied using techniques of segmentation, apodization, multifaceted integrators, and field mapping [1,2]. Refractive, diffractive, and reflective optical components are usually used in existing beam transformation systems. However, all these optical components need careful alignment and their fabrications are complicated and expensive.

In order to overcome the disadvantages of bulk elements and offer compatibility with waveguide resonators and fiber delivery systems, highly multimode (MM) waveguides (usually optical fibers) were used to homogenize the field distribution and generate a flat-top beam profile with circular or square shape [3–5]. However, these techniques were based on incoherent addition of a large number of modes. In addition, special MM fibers (hollow-core, silver-halide, and air-clad square core fibers) have to be developed for these methods and such MM fiber segments must be long enough to achieve the desired flat-top intensity distribution.

Very recently, all-fiber single-mode (SM) Gaussian beam shaping devices are attracting more and more interest since they are not only compact, monolithic, and alignment-free, but also compatible with fiber lasers and fiber delivery systems that have been extensively used in different fields. Most importantly, the beam transformations are accomplished in a coherent approach. Several techniques have been reported in the literature. A long-period fiber Bragg grating (FBG) [6] and an abrupt SM fiber taper [7] have been used to generate top-hat beam profiles in the Fresnel diffraction region. However, the first method requires special equipments to fabricate the grating and is limited to discrete wavelengths and the manufacturing process of fiber tapers used in the second method is hard to control and lacks reproducibility. In [8], a simple all-fiber beam shaper consisting of a short piece of large-core MM fiber and an SM signal delivery fiber was proposed. However, only ring-shaped intensity profiles have been generated within a distance of less than 100 μm away from the MM fiber facet. In fact, substantial experiments on similar fiber devices show that nondiffracting beam is more likely to be generated in the Fresnel range when large-core MM fibers were used [9]. In this paper, detailed investigations on beam transformations using the same fiber structure as in [8] and [9] are completed. It is found that, the core diameter of the MM fiber actually plays an important role in determining the performance of such an all-fiber beam shaper and various beam intensity profiles including top-hat, donut-shaped, taper-shaped, and Bessel-like can be generated when the MM fiber core diameter is of medium size. Moreover, the desired intensity distributions can be generated in free space at a large range of distances from the fiber facet, i.e. in the Fresnel or the Fraunhofer diffraction range, or even in both ranges.

The operating principles of the long-period FBG and fiber taper beam shaping techniques are actually similar to the simple, easy to control, and cost-effective method investigated in this paper. All methods use a special fiber device to excite multiple modes in the fiber cladding [6,7] or directly in the MM fiber core via mode decomposition at the interface between an SM and an MM fibers [8,9]. In all cases an input Gaussian field is transformed to a specific field on the output facet of the MM fiber due to multimode interference (MMI). Diffraction of this confined field produces a desired intensity profile in free space. However, a general description of the physics of these all-fiber beam transformers is not available in the

#120821 - $15.00 USD Received 7 Dec 2009; revised 23 Feb 2010; accepted 28 Feb 2010; published 26 Mar 2010

literature. Moreover, to date beam profiles were investigated only in the Fresnel range close to the fiber output facet and a complete characterization of these beam transformers has not been performed yet. In this paper, the theory of beam transformations based on MMI in optical fiber is presented and the performance of beam shapers fabricated by directly splicing a short piece of MM fiber to an SM signal delivery fiber is investigated in great detail to provide guidelines for real world implementations of aforementioned all-fiber beam shapers [6–9].

The paper is organized as follows; first, the operating principle of coherent beam transformations using MM waveguides is described. Second, the properties and characteristics of beam transformations are investigated in detail through theoretical calculations. Third, the experimental results of coherent laser beam transformations using a short piece of MM fiber are presented to confirm the analytical results.

2. Principle of coherent beam transformations using multimode waveguides

In this section, the operating principle of coherent beam transformations using MM waveguides is presented. In contrast to incoherent homogenization using a long highly MM waveguide, only a short piece of MM waveguide (one centimeter long or shorter) is used for MMI-based beam transformations. Moreover, coherence of the shaped beam is still maintained. Although multiple modes can be excited in an MM waveguide via different approaches such as mode mismatching [8,9], Bragg grating [6], and waveguide taper [7], a basic configuration depicted in Fig. 1 is used to illustrate the approach in general and provide universal insight of beam transformations using MM waveguides.

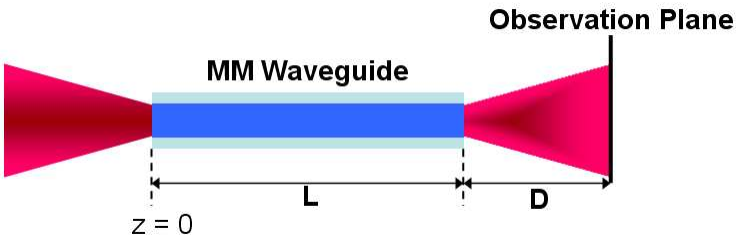

Fig. 1. Schematic depiction of beam transformation using MM waveguides.

We assume that a field $E_{in}(x, y, z = 0)$ is launched to an MM waveguide with a length of L, as shown in Fig. 1. The incident field can be decomposed into guided modes of the MM waveguide, i.e.,

$$E_{in}(x, y, z = 0) = \sum_{1}^{M}\sum_{1}^{N} C_{mn} e_{mn}(x, y, z = 0), \tag{1}$$

where $e_{mn}(x, y, z = 0)$ is the *mn*-th guided mode of the MM waveguide. M×N is the number of excited modes inside the MM fiber. C_{mn} is the mode expansion coefficient and can be determined from

$$C_{mn} = \frac{\iint_S E_{in}(x, y, 0) \times e^{*}_{mn}(x, y, 0) ds}{\iint_S \left| e_{mn}(x, y, 0) \right|^2 ds}. \tag{2}$$

All excited modes propagate independently inside the MM waveguide, and the field on the output facet of the MM fiber is the superposition of excited modes and can be written as

$$E_{out}(x, y, L) = \sum_{1}^{M}\sum_{1}^{N} C_{mn} e_{mn}(x, y, 0) e^{-i\beta_{mn} L}, \tag{3}$$

where β_{mn} is the propagation constant of the *mn*-th excited mode of the MM waveguide.

#120821 - $15.00 USD Received 7 Dec 2009; revised 23 Feb 2010; accepted 28 Feb 2010; published 26 Mar 2010

According to Eq. (3), the field distribution at the facet of the MM waveguide depends on the waveguide length (L), the decomposition coefficient, which is determined by the ratio (R) between the mode size of the incident field and the cross section dimension of the MM waveguide, and the propagation constant, which is wavelength (λ) dependent. Thus, a large variety of fields confined to the MM waveguide can be created at the output facet by controlling the three variables L, R, and λ. Diffraction of these confined fields produces various intensity profiles in free space. In principle, any desired intensity profile can be generated at any distance from the waveguide facet in free space if its corresponding facet field is obtained through a precise waveguide design.

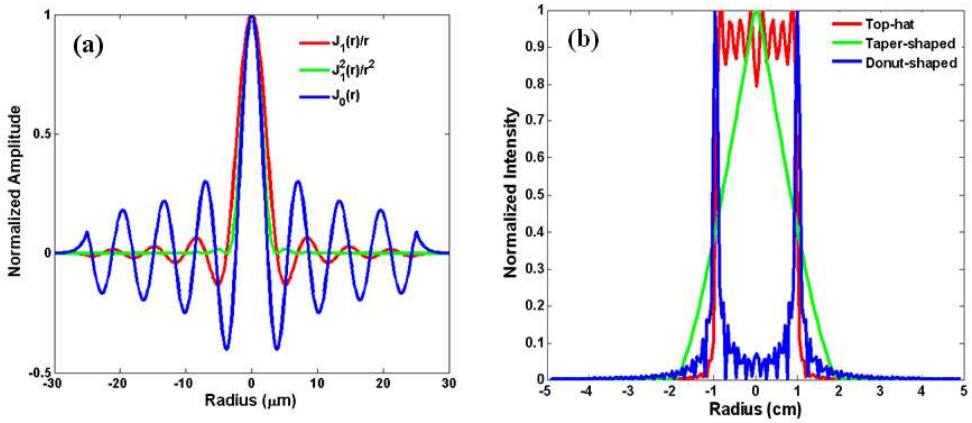

Fig. 2. (a) Distributions of three considered facet fields of a 50 μm cylindrical waveguide and (b) their corresponding far-field intensity profiles. Top-hat (red); taper-shaped (green); donut-shaped (blue).

For cylindrical waveguides such as MM optical fibers, many desired intensity profiles with circular symmetry including top-hat, donut-shaped, taper-shaped, and Bessel-like can be obtained through proper design of the MM waveguide and tuning the input signal wavelength. According to Fraunhofer diffraction theory, any intensity profile mentioned above can be obtained in the far-field if a field corresponding to its inverse Fourier transformation is generated at the output facet of the MM waveguide. For instance, as shown in Fig. 2, if a field with an Airy disc distribution described by $J_1(r)/r$ [where $J_1(r)$ is the first order Bessel function, red curve in Fig. 2(a)] is generated at the facet, a top-hat far-field intensity profile with steep edges [red curve in Fig. 2(b)] can be obtained. A taper-shaped intensity profile [green curve in Fig. 2(b)] is generated in the far-field when the facet field is described by $J_1^2(r)/r^2$ [green curve in Fig. 2(a)]. A donut-shaped far-field pattern [blue curve in Fig. 2(b)] can be created when a facet field with a Bessel distribution described by $J_0(r)$ [where $J_0(r)$ is the zeroth order Bessel function, blue curve in Fig. 2(a)] is generated; and inversely, a Bessel far-field pattern can be produced from a facet field with a donut-shaped distribution. Note that the ripples on the far-field intensity profiles are due to the finite facet fields that are confined in the considered waveguide with a diameter of 50 μm.

3. Beam transformations using multimode optical fibers

Optical fibers have been extensively used to deliver high intense laser beam to the work place with great operational flexibility and minimal energy loss. Straightforwardly, beam transformers using MM optical fibers are not only highly compatible with the fiber delivery system, but also alignment-free, compact, cost effective, and easy to fabricate. In this section, beam transformations using MM fibers are thoroughly investigated through theoretical calculations.

#120821 - $15.00 USD Received 7 Dec 2009; revised 23 Feb 2010; accepted 28 Feb 2010; published 26 Mar 2010

3.1 An all-fiber beam transformer

Here, an all-fiber device (shown in Fig. 3) that was fabricated by splicing a short piece of MM fiber to an SM delivery fiber is used to investigate the properties of beam transformations using MM optical fibers. Compared to designs using FBGs and fiber tapers, this design is simple, cost effective, and robust. The conclusions, however, are universal and can be applied to all fiber-optic beam shapers that have been already demonstrated and even free space coupled MM fiber segment as shown in Fig. 1.

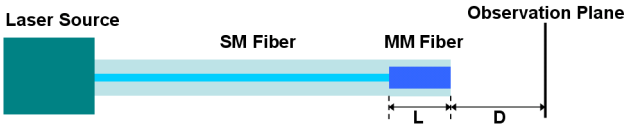

Fig. 3. Design of an all-fiber device for laser beam shaping (the figure is not to scale).

Since there already have been some investigations on MMI in similar fiber structures for different applications [10–16], here, we only describe the basics of the operation principle of the fiber device. The fundamental $LP_{0,1}$ mode [$E_{in}(r, \phi)$] of the SM fiber is coupled to the MM fiber where $LP_{0,n}$ modes [$e_n(r, \phi)$, n is the radial index] are excited exclusively due to symmetric on-axis excitation and mode orthogonality. Each $LP_{0,n}$ mode propagates along the fiber independently with its own propagation constant. Similar to Eq. (3), the field at the output facet of the MM fiber can be written as

$$E_{Out}(r,\varphi,L)=\sum_{n=1}^{N}C_n e_n(r,\varphi)e^{-i\beta_n L}, \tag{4}$$

To investigate the characteristics of this fiber device, the free space propagation of the beam exiting the monolithic fiber device that consists of a conventional SM fiber (SMF-28) and an MM fiber is calculated. The field distributions in observation planes between 1 mm and 20 mm away from the fiber facet are obtained using Fresnel diffraction in cylindrical coordinates [6]:

$$E_{fs}(r,\varphi)=\frac{1}{i\lambda D}e^{i\frac{\pi r^2}{\lambda D}}\iint_{S'}E_{out}(r',\varphi')e^{i\frac{\pi r'^2}{\lambda D}}J_0\left(\frac{2\pi r' r}{\lambda D}\right)ds', \tag{5}$$

where r' and ϕ' are the coordinates at the fiber facet, and D is the distance from the observation plane to the fiber facet. The field distributions in the near-field planes with a distance less than 1 mm have been calculated using the transfer function in free space [17]:

$$E_{fs}(r,\varphi)=FT^{-1}\left\{FT\left[E_{out}(r',\varphi')\right]\exp\left[i\frac{2\pi D}{\lambda}\sqrt{1-(\lambda\xi)^2-(\lambda\eta)^2}\right]\right\}, \tag{6}$$

where ξ and η are spatial frequencies of the facet field and FT and FT^{-1} represent a 2-dimensional Fourier transformation and an inverse Fourier transformation, respectively.

The fully vectorial mode expansion approach, developed by Li [18], is used to do the calculation of C_ns in Eq. (4) and determine the facet field E_{out}. Near-field and far-field intensity profiles are obtained by calculating the diffraction of the confined facet field using Eqs. (5) and (6), respectively. Beam transformations using MM fibers with a NA of 0.22 and core diameters of 25 μm, 50 μm and 105 μm are investigated.

3.2 Beam shaping of an all-fiber beam transformer

In our investigations, 50-μm-diameter fiber is found to exhibit better performance versatility than 25 μm and 105 μm fibers when the delivery fiber is an SMF-28 fiber (core diameter of 8.2 μm and NA of 0.14). Therefore, results of 50 μm fiber are mainly presented to demonstrate the beam shaping properties of the all-fiber beam transformer depicted in Fig. 3.

#120821 - $15.00 USD Received 7 Dec 2009; revised 23 Feb 2010; accepted 28 Feb 2010; published 26 Mar 2010

Considering a 50 μm MM fiber segment with 10 mm length and the signal wavelength of 1572 nm, the intensity distribution of the beam at selected planes in free space is plotted in Fig. 4. Clearly, in this case a top-hat beam is generated in both the Fresnel and the Fraunhofer diffraction regions starting from 800 μm. In contrast, when the signal wavelength is 1580 nm, a top-hat beam can be generated only in Fresnel region of 500-1000 μm near the fiber facet as shown in Fig. 5. Therefore, the plane where a desired beam profile is created can be varied by changing the signal wavelength. In addition, according to the properties of MMI in MM waveguides [9,10,16], the location of a desired beam profile can also be varied by changing the length of the MM fiber. In other words, a desired intensity profile in the far-field region can be shifted to the near-field region by changing the signal wavelength or the length of the MM fiber. Thus, far-field intensity profiles are mainly considered in this paper.

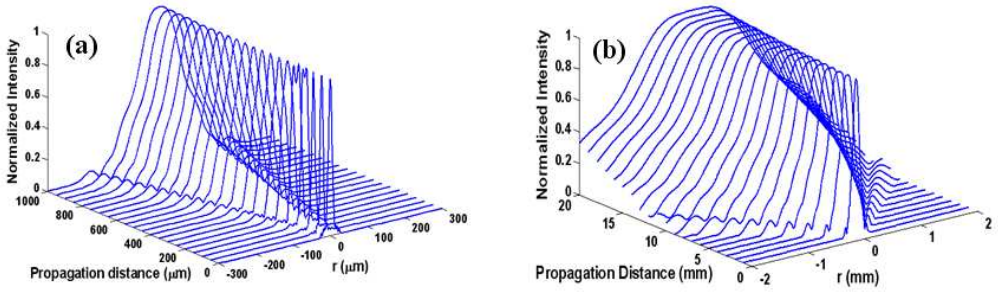

Fig. 4. Intensity distribution of the laser beam propagating in free space when the signal wavelength is 1572 nm. (a) The plot ranges from 1 mm to 20 mm; (b) the plot ranges from 0 mm to 1 mm.

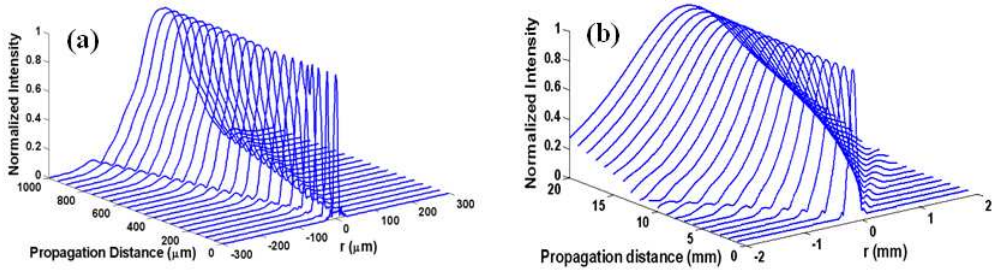

Fig. 5. Intensity distribution of the laser beam propagating in free space when the signal wavelength is 1580 nm. (a) The plot ranges from 1 mm to 20 mm; (b) the plot ranges from 0 mm to 1 mm.

For the case of beam transformation shown in Fig. 4, where the signal wavelength is 1572 nm, the intensity profile of the top-hat beam at a distance of 20 mm from the MM fiber facet is redrawn by the red line in Fig. 6(a). This top-hat beam has gradually sloped edges because the field at the fiber facet [shown by the red curve in Fig. 6(b)] deviates from an ideal Airy disc distribution [shown by the red curve in Fig. 2(a)]. As the signal wavelength changes to 1525 nm, a donut-shaped beam is created. Its intensity distribution and the corresponding facet field are plotted as blue curves in Fig. 6(a) and 6(b), respectively. Although the facet field is far from an exact Bessel distribution [shown by the blue curve in Fig. 2(a)], a donut-shaped distribution with a nonzero center can still be generated in the far-field region because the two rings that compose the facet field are out of phase and their diffractions at the central region are partially destructive. Note that, a donut-shaped intensity profile with a zero center can be more easily obtained when the 105 μm MM fiber is used because in a larger core it is easier to generate a facet field close to a Bessel distribution. When the signal wavelength changes to 1559 nm, a taper-shaped far-field is created. The intensity profile and its corresponding facet field are plotted as green curves in Fig. 6 (a) and 6(b), respectively.

#120821 - $15.00 USD Received 7 Dec 2009; revised 23 Feb 2010; accepted 28 Feb 2010; published 26 Mar 2010

When the length of the MM fiber segment is changed from 10 mm to 11 mm the performance of the fiber device is different. A Bessel-like beam with a low-divergence central spot is always generated. For a signal wavelength of 1555 nm the intensity profile of the Bessel-like beam at a distance of 20 mm and its corresponding facet field are plotted by black curves in Fig. 6(a) and 6(b), respectively. Although the facet field is not a perfect donut, the far field still closely resembles a Bessel-like beam because the two rings of the facet field are out of phase with the central spot and their destructive diffractions cut down the peripheral distribution.

Based on the calculation results of the 50 μm MM fiber above, it is reasonable to draw a conclusion that beam transformations based on MMI exhibit a versatile functionality and most desired beams can be obtained at any plane in free space by changing the parameters that determine the facet field, i.e. the signal wavelength, the length of the MM fiber segment, and the core diameter of the MM fiber segment. In the next three subsections, performance dependence of an all-fiber beam transformer on the three parameters is discussed, respectively.

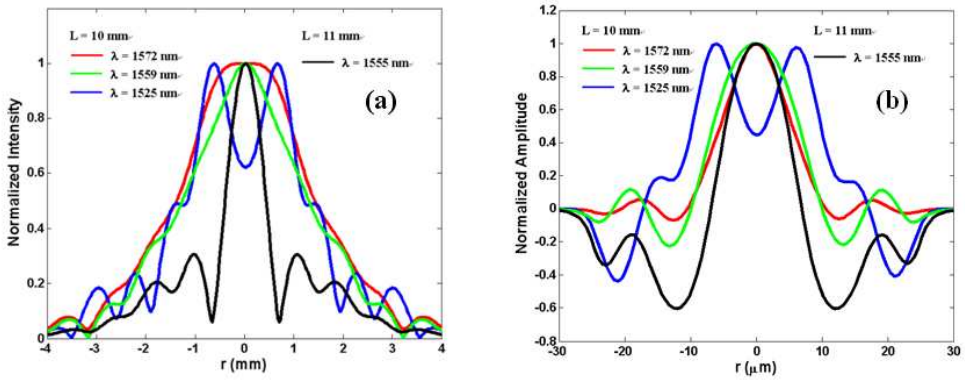

Fig. 6. (a) Four often desired intensity profiles generated at a distance of 20 mm from the fiber facet and (b) the corresponding field distribution at the MM fiber facet. Red curve (top-hat); green curve (taper-shaped); red curve (donut-shaped); black curve (Bessel-like).

3.3 Wavelength dependence of an all-fiber beam transformer

Since the facet field E_{out} (r, ϕ, L) expressed by Eq. (4) depends on the signal wavelength through the dispersion of the propagation constant, different desired intensity profiles can be obtained by just tuning the signal wavelength. On the other hand, a stable performance of a beam transformer resorts to a weak wavelength dependence that can also lower the requirements regarding the signal source. As analyzed in refs [10,16], the wavelength dependence can be manipulated by selecting a proper MM fiber length because the phase term in Eq. (4) is directly related to the length of the MM fiber segment. A beam transformer using a long MM fiber can provide a fast variation of the intensity profile with changing signal wavelength. Wavelength-stable performance can be obtained when a short MM fiber segment is used. Therefore, there is a tradeoff between the tunability and the stability of an all-fiber beam transformer.

In this section, wavelength dependence of the beam transformers considered in the previous subsection is discussed. Considering the wavelength range of a readily available signal source at optical telecommunication window, our calculations are carried out within a wavelength range of 1500-1600 nm.

Our calculations show that top-hat beams can be obtained in the far-field region for wavelengths between 1564 nm and 1574 nm when the MM fiber length is 10 mm. The intensity profiles at a 20 mm distance away from the MM fiber facet are plotted in Fig. 7(a). Within the 10 nm wavelength range, a flat-top intensity profile is always achievable. For

#120821 - $15.00 USD Received 7 Dec 2009; revised 23 Feb 2010; accepted 28 Feb 2010; published 26 Mar 2010

wavelengths longer than 1574 nm, the top width of the far-field profile becomes narrow slowly but top-hat beams can be created in the near-field region like the case of 1580 nm shown in Fig. 5. As the wavelength is shorter than 1564 nm, the top of the far-field profile becomes sharp quickly and changes to a taper-shaped far-field profile at a wavelength of 1559 nm as shown in Fig. 7(b). Seen from Fig. 7(b), the taper-shaped intensity profile shows strong wavelength dependence, i.e., 1 nm wavelength difference can result in a large deviation from a taper-shaped intensity profile.

It is also found that a donut-shaped far-field distribution can be obtained for wavelengths between 1520 nm and 1545 nm. More specially, in a wavelength range of 1525-1530 nm, the donut-shaped intensity profile at a 20 mm distance show little variation as shown in Fig. 7(c). At other wavelengths, normalized intensities of the beam centers are larger than 0.6.

When the MM fiber length is 11 mm, Bessel-like beams can always be created in the far-field region for the considered wavelength range of 1500-1600 nm as shown in Fig. 7(d). The low-divergence of the Bessel-like beam results in a far-field intensity profile with a full-width at half maximum (FWHM) of only 0.823 mm at a 20 mm distance from the MM fiber facet.

With the advances of laser technologies, a wavelength-tunable signal with a linewidth of less than 0.01 nm is readily available. Therefore, an all-fiber beam transformer can not only work with a large tunablility but also a high stability.

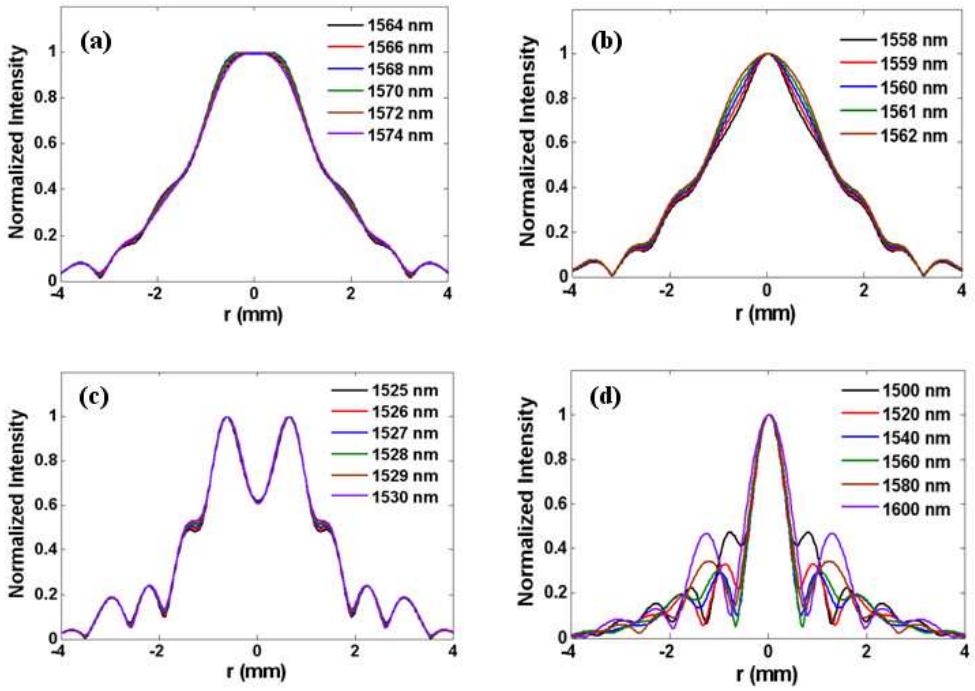

Fig. 7. Wavelength dependence of the fiber-optic beam transformer for the four cases shown in Fig. 5. (a) Top-hat, (b) taper-shaped, (c) donut-shaped, and (d) Bessel-like.

3.4 Length dependence of an all-fiber beam transformer

As stated in subsection 3.3, wavelength stable performance of a fiber-optic beam transformer depends on the length of the MM fiber segment. On the other hand, the facet field E_{out} (r, ϕ, L) expressed by Eq. (4) is directly related to the MM fiber length. Therefore, performance of a beam transformer is strongly determined by the MM fiber length. For a signal with a certain wavelength, according to the phase term in Eq. (4), a desired intensity profile can be obtained by cleaving the MM fiber segment with a proper length [16]. For instance, when the signal wavelength is 1535 nm, a top-hat intensity profile can be obtained at a 20 mm distance from

#120821 - $15.00 USD Received 7 Dec 2009; revised 23 Feb 2010; accepted 28 Feb 2010; published 26 Mar 2010

the fiber facet when the MM fiber length is 10.2 mm. As the MM fiber length changes to 10.26 mm, a taper-shape intensity profile in the far-field region is created. A donut-shaped distribution with a nonzero center is generated in the far-field when the MM fiber length is 10.61 mm. And low divergence Bessel-like intensity profile is always attainable for an MM fiber length of about 11mm. In this subsection, length dependence of the all-fiber beam transformer is discussed for the four cases.

In Fig. 8(a), far-field intensity profiles are plotted for MM fiber lengths between 10.18 mm and 10. 24 mm. A top-hat intensity profile with a good flatness can be achieved within 60 μm length range. Using common equipments in laboratory, an optical fiber can be cleaved with an accuracy of better than 10 μm for a total length shorter than 100 mm [14,16]. Thus, it's easy and reliable to fabricate an all-fiber beam transformer that transforms a Gaussian beam to a top-hat beam for a desired wavelength. See the intensity profiles shown in Fig. 8(b), producing a taper-shaped beam would be a little challenging since a 10 μm length difference leads to an observable deviation from the linear slope edges that are only obtained for 10.26 mm long MM fiber. However, it's still attainable for a total length of about 10 mm with recent fiber technology.

Donut-shaped intensity profiles can be obtained when the MM fiber length is between 10.6 mm and 10.64 mm [shown in Fig. 8(c)]. Little variation of the intensity profiles when the MM fiber length changes from 10.61mm to 10.63 mm. Comparing to top-hat, taper-shaped, and donut-shaped beams, Bessel-like beams are very easy to be obtained from an all-fiber beam transformer because low divergence beams with an FWHM of less than 0.8 mm can be created for an MM fiber length between 10.75 mm and 11.45 mm as shown in Fig. 8(d).

Based on the evolution of the intensity profiles with the MM fiber length shown in Fig. 8, it can be concluded that, for a signal with a certain wavelength, most desired beams can be generated by precisely control of the MM fiber length.

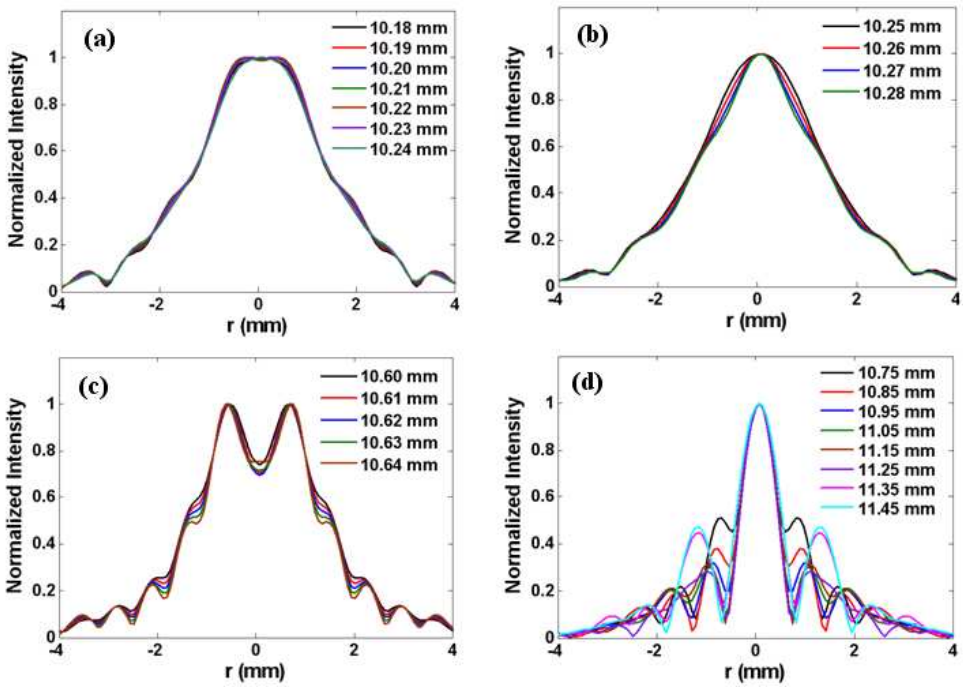

Fig. 8. Far-field intensity profiles at a 20 mm distance from the MM fiber facet for all-fiber beam transformers with different MM fiber lengths. (a) Top-hat; (b) taper-shaped; (c) donut-shaped; (d) Bessel-like.

#120821 - $15.00 USD Received 7 Dec 2009; revised 23 Feb 2010; accepted 28 Feb 2010; published 26 Mar 2010

3.5 Core-size dependence of an all-fiber beam transformer

According to Eq. (4), the facet field distribution E_{out} (r, ϕ, L) also depends on the mode expansion coefficients that are determined by the ratio of the core diameter between the SM delivery fiber and the MM fiber. Therefore, performance of an all-fiber beam transformer is much related to the core size of the MM fiber. In this subsection, intensity profiles of the most desired beams generated from beam transformers using MM fibers with NA of 0.22 and core diameters of 25 μm, 50 μm, and 105 μm are compared and analyzed.

When the signal delivery fiber is an SMF-28 fiber, energy percentages of the excited modes in the MM fibers with core diameters of 25 μm, 50 μm, and 105 μm are plotted in Fig. 9, respectively. Only first four linear polarized (LP) modes are excited in the 25 μm MM fiber and most energy is contained in the first two modes. With such a mode constitution, a facet field that generates a donut-shaped beam in far-field region is never reformed from the input Gaussian beam. Thus, donut-shaped beams cannot be generated from this beam transformer. When the 50 μm MM fiber is used, first seven LP modes are excited. As analyzed above, most desired beams can be obtained from this beam transformer. First thirteen LP modes are excited in the 105 μm MM fiber and energy distribution is more even than that of 25 μm and 50 μm. Due to the complicated interference of such a large number of modes, a taper-shaped beam that is originated from a simple facet field distribution [green curve in Fig. 2(a)] is hard to be obtained from the 105 μm MM fiber.

Intensity profiles of the top-hat beams with the widest top generated from MM fibers with diameters of 25 μm, 50 μm and 105 μm are plotted in Fig. 10(a), respectively. When the core diameter is 25 μm or 50 μm, the top-hat intensity profile is much smoother and has a good flat top. For the 105 μm MM fiber, however, both smoothness and flatness are degraded because of the ring-shaped far-field of high order LP modes [9]. Therefore, small-core MM fibers are preferred for top-hat beam generation.

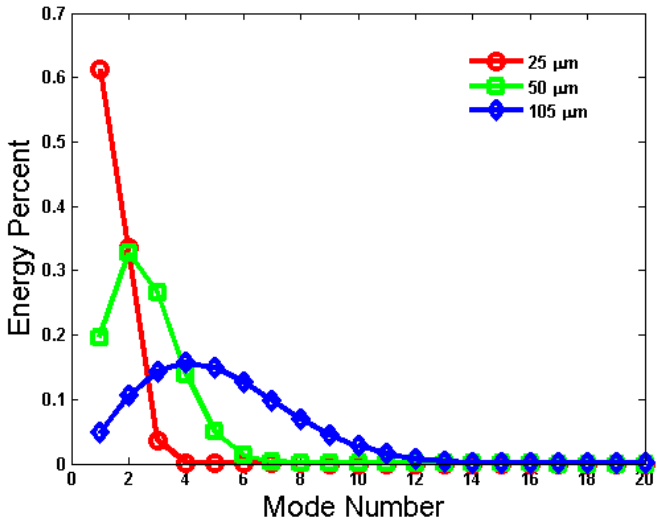

Fig. 9. Energy percentages of the excited modes in the MM fibers with diameters of 25 μm (red circles), 50 μm (green squares), and 105 μm (blue diamonds), respectively, when the signal delivery SM fiber is SMF-28.

#120821 - $15.00 USD Received 7 Dec 2009; revised 23 Feb 2010; accepted 28 Feb 2010; published 26 Mar 2010

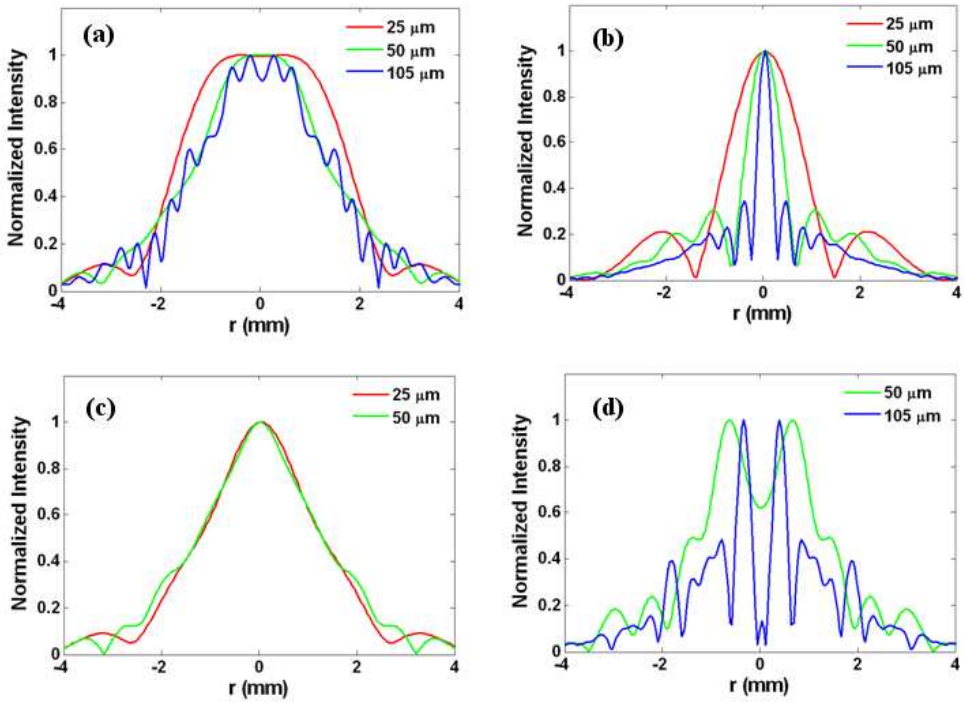

Fig. 10. Comparisons of the far-field intensity profiles of the desired beams generated from beam transformers using 25 μm, 50 μm, and 105 μm MM fibers, respectively. (a) top-hat; (b) Bessel-like; (c) taper-shaped; (d) donut-shaped.

Contrarily, larger core MM fiber is preferred for non-diffracting beam generation [9]. As shown in Fig. 10(b), Bessel-like beam generated from the 105 μm MM fiber has the smallest central peak. The FWHM of the Bessel-like beam generated from the 105 μm MM fiber is only one seventh of that of the Bessel-like beam generated from the 25 μm MM fiber.

Taper-shaped beams generated from the 25 μm and 50 μm MM fibers are plotted in Fig. 10(c). The beam profile from the 25 μm MM fiber resembles closer a real taper-shape than that from the 50 μm MM fiber. Because the narrow facet field that generates a taper-shaped beam [shown by green curve in Fig. 2(a)] cannot be obtained from multimode interference, taper-shaped intensity profiles are hard to be obtained from the 105 μm MM fiber. Therefore, small-core MM fibers are necessary for the generation of almost taper-shaped beams.

The intensity profiles of donut-shaped beams generated from the 50 μm and 105 μm MM fibers are plotted in Fig. 10(d). In contrast to the beam with a nonzero center coming from the 50 μm fiber, a donut-shaped profile with a zero center can be obtained from the 105 μm MM fiber. Moreover, the ring of the beam generated from the 105 μm MM fiber is much thinner than that of the beam generated from the 50 μm MM fiber. Donut-shaped beams are difficult to obtain from 25 μm MM fiber since more than 95% of the energy is contained in the LP_{01} and LP_{02} modes. Thus, large core MM fibers are needed for generating donut-shaped beams.

4. Experimental results of beam transformations using multimode optical fibers

Experimental investigations of beam transformations using MM optical fibers were accomplished with the monolithic fiber device that is schematically shown in Fig. 3. A short-piece of MM fiber is directly spliced onto an SM signal delivery fiber. Since the performance of this fiber device can be manipulated through the wavelength of the launched light as analyzed above, a single-frequency semiconductor laser (Agilent, Model 81680A) with a wavelength tuning range from 1456 nm to 1584 nm was applied as the signal source. An

#120821 - $15.00 USD Received 7 Dec 2009; revised 23 Feb 2010; accepted 28 Feb 2010; published 26 Mar 2010

infrared CCD camera (Electrophysics, Model 7290 A) was used to record the intensity profiles in observation planes.

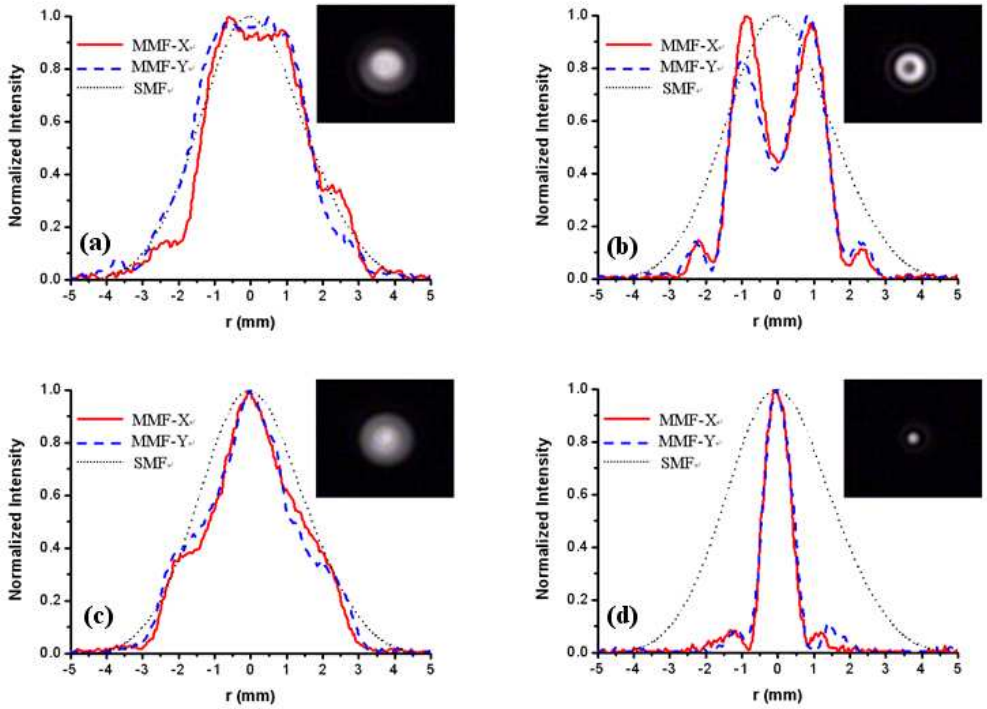

Fig. 11. (a) top-hat, (b) donut-shaped, (c) taper-shaped, and (d) Bessel-like intensity profiles created experimentally and recorded by a CCD camera at a distance of 20 mm from the MM fiber facet. (For comparison, the intensity profile of the beam exiting directly from the SM fiber is also plotted.).

Experiments were firstly carried out with several pieces of 50 μm MM fiber with lengths around 10 mm in approximation of the idealized simulation studies. The generated intensity patterns were recorded by a CCD camera at a 20 mm distance from the MM fiber facet and prominent examples are shown in Fig. 11. For comparison, the far-field intensity profile of light exiting directly from the SM fiber is included. When the MM fiber length is 10 mm and the signal wavelength is between 1556 nm and 1568 nm, a top-hat beam can be created. At a wavelength of 1561 nm, the top-hat beam has the widest top. Its intensity profile and image are shown in Fig. 11(a). The uniformity of the top-hat beam in the central 1.8 mm is within a few percent when it is measured by a scanning slit of 2 μm width. In contrast, a donut-shaped beam is obtained as the signal wavelength changes to 1515-1523 nm and 1478-1496 nm. When the signal wavelength is 1482 nm, a donut-shaped with the lowest central intensity is obtained and is shown in Fig. 11(b). Although a taper-shaped beam is created when the wavelength is 1550 nm and the MM fiber length is 10mm, a taper-shaped beam with a much better linear slope [shown in Fig. 11(c)] is obtained when the MM fiber length is 10.1 mm and the signal wavelength is 1567 nm. Finally, a low-divergence Bessel-like beam with the highest central intensity is obtained [shown in Fig. 11(d)] when the MM fiber length is 10.9 mm and the signal wavelength is 1534 nm. In this case, the divergence angle of the central spot is less than a fourth of that of the input Gaussian beam. Clearly, the experimental results indicate the functionality and high versatility of this simple fiber device. Slightly deviating features in the intensity distributions can be attributed to imperfect connections between SM fiber and MM fiber segments as well as interference effects occurring at the detector plane of the CCD camera.

#120821 - $15.00 USD Received 7 Dec 2009; revised 23 Feb 2010; accepted 28 Feb 2010; published 26 Mar 2010

In order to show the advantages of large-core MM fibers for generating donut-shaped and Bessel-like beams, several pieces of 105 μm MM fiber with lengths from 10 mm to 15 mm with a step of 1 mm and from 20 mm to 40 mm with a step of 5 mm were investigated. It is found that Bessel-like beam is generated frequently from 105 μm MM fibers. More specially, Bessel-like beam is always created through out the available wavelengths of the signal source when the MM fiber length is 12 mm and 13 mm. The intensity profile of a typical Bessel-like beam is plotted in Fig. 12(a). When the MM fiber length is 25 mm, a donut-shaped beam with a zero center is generated for the signal wavelengths between 1590 nm and 1560 nm. The intensity profile of a typical donut-shaped beam is shown in Fig. 12(b). Obviously, the donut-shaped beam not only has a zero center, but also has a thinner the ring comparing to the donut-shaped beam shown in Fig. 11(b).

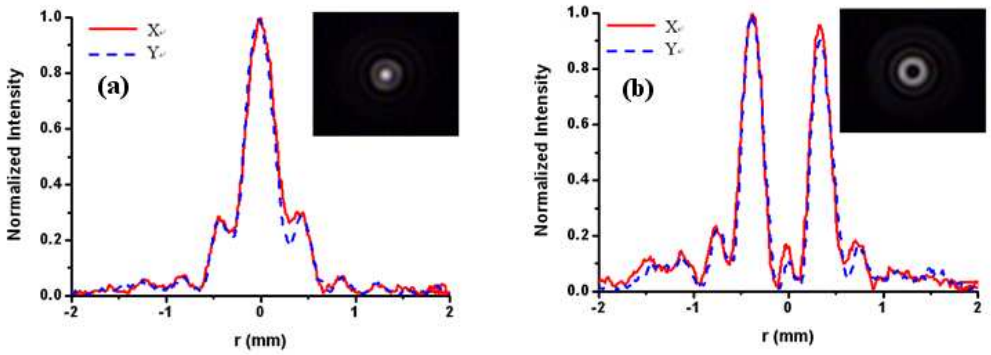

Fig. 12. (a) Bessel-like and (b) Donut-shaped intensity profiles created experimentally and recorded by a CCD camera at a distance of 20 mm from the 105 μm MM fiber facet.

With the advances of high power fiber lasers and amplifiers, large-mode-area (LMA) SM fibers are usually used to suppress nonlinear effects and scale up the handling power. In order to evaluate the high compatibility of an all-fiber beam transformer with recent high power fiber laser and amplifier systems, a beam transformer using an LMA SM fiber and a 105 μm MM fiber is investigated. The passive SM fiber has a core diameter of 10 μm and a NA of 0.07 (i.e., about 23 μm of the mode-field diameter).

#120821 - $15.00 USD Received 7 Dec 2009; revised 23 Feb 2010; accepted 28 Feb 2010; published 26 Mar 2010

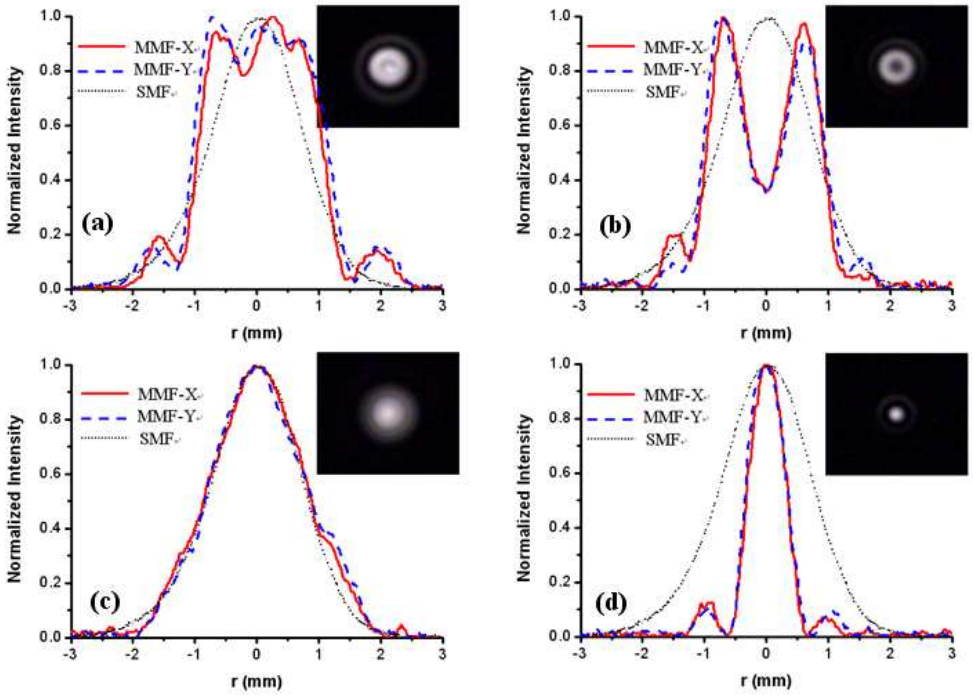

Fig. 13. (a) top-hat, (b) donut-shaped, (c) taper-shaped, and (d) Bessel-like intensity profiles created experimentally and recorded by a CCD camera at a distance of 20 mm from a beam transformer consisting of a 105 μm MM fiber and an SM fiber with a mode-field diameter of 23 μm. (For comparison, the intensity profile of the beam exiting directly from the LMA SM fiber is also plotted.).

When the MM fiber is 14.5 mm long, the performance of this beam transformer is similar to that of the beam transformers using an SMF-28 fiber. A top-hat beam with the widest top is obtained when the signal wavelength is 1558 nm. Its intensity profile and its image at a 20 mm distance from the MM fiber facet are shown in Fig. 13(a). When the wavelength is 1492 nm, a donut-shaped beam with its intensity profile and its image as shown in Fig. 13(b) is obtained. A taper-shaped beam [shown in Fig. 13(c)] is created in the far-field region when the signal wavelength is 1546 nm. As the MM fiber length changes to 10 mm, Bessel-like beam can be obtained in a wavelength range from 1550 nm to 1580 nm. The intensity profile and the image of a Bessel-like beam for a signal at 1562 nm are shown in Fig. 13(d). The experimental results demonstrate that all desired beams can also be generated from the 105 μm MM fiber when the SMF has a mode-field diameter of 23 μm. Note that, the mode-field diameter of the SM delivery fiber can be even much larger referring to recent fiber fabrication technology, then the 105 μm MM fiber may not be competent for the generation of donut-shaped beams and an MM fiber with a larger core diameter will be needed.

5. Discussion and conclusion

Beam shaping based on MMI is a coherent beam transformation in contrast to incoherent beam homogenizing using a long highly MM waveguides. Due to the interference of the excited modes, an input beam can be transformed to a specific field on the MM waveguide facet. Diffraction of the confined facet field can generate desired beams in free space. Our calculations show that, in addition to generating a top-hat beam like a beam homogenizer does, a short piece of cylindrical MM waveguide can transform an input Gaussian beam to a donut-shaped, a taper-shaped, or a Bessel-like beam. Comparing to beam homogenizers, beam transformers based on MMI exhibit superior functionality and high versatility. It should be

#120821 - $15.00 USD Received 7 Dec 2009; revised 23 Feb 2010; accepted 28 Feb 2010; published 26 Mar 2010

noted that the input beam can be of any distribution other than Gaussian as long as a desired field can be formed at the output facet of the MM waveguide.

Analysis and characterization of a simple and compact all-fiber beam transformer show that an input Gaussian beam can be transformed to various desired beams. The performance of this fiber device can be easily and widely manipulated through parameters including the length of the MM fiber segment and the ratio between the core diameters of the MM and the SM fiber segments. Desired beams can also be obtained for a certain wavelength by precisely tailoring the MM fiber. When the core ratio is small, a small number of modes are excited in the MM fiber. Top-hat and taper-shaped beams are more likely to be obtained in this case. When the ratio is large, a large number of modes are excited in the MM fiber and formation of top-hat or taper-shaped beams rarely occur. However, donut-shaped beams with a zero center can be exclusively generated from a large-core MM fiber. Moreover, diffraction of a desired beam is more limited when the beam is generated by a large core MM fiber rather than a small core fiber.

Due to the dispersion of the propagation constants, the intensity profile of an output beam as well as its location can be controlled by tuning the signal wavelength. It is worth mentioning that, the desired intensity profiles can be generated in the Fresnel or the Fraunhofer diffraction range, or even in both ranges. In particular, parallel desired beam profiles can be obtained by using a fiber collimator if they are formed in the far-field region. This provides an easy and effective method to manipulate the performance of the beam transformer even after the device has been fabricated. Wavelength-based variability of the beam transformation is tightly related to the length of the MM fiber. Varying of the beam intensity profile with the signal wavelength is fast as the MM fiber is long. When the MM fiber is short, an intensity profile can be maintained in a large wavelength range. Therefore, in addition to compactness, a tradeoff between wavelength tunability and profile stability of a beam transformer should be considered when the MM fiber length is selected.

Beam transformation techniques using MM fibers enable compact, monolithic, and alignment-free all-fiber beam shaping devices with high flexibility and minimal loss that are highly compatible with high power fiber lasers and amplifiers systems and fiber delivery systems. Our experimental results using commercial MM fibers agree well with the calculations. Desired beams with much better distributions that are required for some specific applications can be achieved if the MM fiber segments are precisely designed or modulated by inscribing long-period FBGs in the cores.

6. Summary

We have provided physical insight to coherent beam transformations using multimode waveguides. Our calculations and experimental results confirm the superior functionality of beam transformations using MM optical fibers. While analyses and experimental investigations in this paper have been focusing of rather simple and well-controllable all-fiber beam transformers, the results and conclusions are applicable to a large variety of beam shaping techniques based on MMI in MM waveguides.

Acknowledgments

This work is supported by the National Sciences Foundation through grant No. 0725479 and the state of Arizona TRIF Photonics Initiative.

#120821 - $15.00 USD Received 7 Dec 2009; revised 23 Feb 2010; accepted 28 Feb 2010; published 26 Mar 2010